Energy principle for excitations in plasmas with counterstreaming electron flows

Cite as: AIP Advances **8**, 055213 (2018); https://doi.org/10.1063/1.5008254
Submitted: 04 October 2017 • Accepted: 03 May 2018 • Published Online: 14 May 2018

Atul Kumar, Chandrasekhar Shukla, Amita Das, et al.

Energy principle for excitations in plasmas with counterstreaming electron flows

Atul Kumar,[a] Chandrasekhar Shukla, Amita Das,[b] and Predhiman Kaw[c]
Institute for Plasma Research, HBNI, Bhat, Gandhinagar 382428, India

(Received 4 October 2017; accepted 3 May 2018; published online 14 May 2018)

A relativistic electron beam propagating through plasma induces a return electron current in the system. Such a system of interpenetrating forward and return electron current is susceptible to a host of instabilities. The physics of such instabilities underlies the conversion of the flow kinetic energy to the electromagnetic field energy. Keeping this in view, an energy principle analysis has been enunciated in this paper. Such analyses have been widely utilized earlier in the context of conducting fluids described by MHD model [I. B. Bernstein *et al.*, Proceedings of the Royal Society of London A: Mathematical, Physical and Engineering Sciences **244**(1236), 17–40 (1958)]. Lately, such an approach has been employed for the electrostatic two stream instability for the electron beam plasma system [C. N. Lashmore-Davies, Physics of Plasmas **14**(9), 092101 (2007)]. In contrast, it has been shown here that even purely growing mode like Weibel/current filamentation instability for the electron beam plasma system is amenable to such a treatment. The treatment provides an understanding of the energetics associated with the growing mode. The growth rate expression has also been obtained from it. Furthermore, it has been conclusively demonstrated in this paper that for identical values of $S_4 = \sum_\alpha n_{0\alpha} v_{0\alpha}^2 / n_0 \gamma_{0\alpha}$, the growth rate is higher when the counterstreaming beams are symmetric (i.e. $S_3 = \sum_\alpha n_{0\alpha} v_{0\alpha} / n_0 \gamma_{0\alpha} = 0$) compared to the case when the two beams are asymmetric (i.e. when S_3 is finite). Here, $v_{0\alpha}$, $n_{0\alpha}$ and $\gamma_{0\alpha}$ are the equilibrium velocity, electron density and the relativistic factor for the electron species 'α' respectively and $n_0 = \sum_\alpha n_{0\alpha}$ is the total electron density. Particle - In - Cell simulations have been employed to show that the saturated amplitude of the field energy is also higher in the symmetric case. https://doi.org/10.1063/1.5008254

I. INTRODUCTION

An intense laser interacting with an overdense solid target generates highly energetic, relativistic electrons carrying a very large electron current (~*MAmps*) in the forward direction.[1–3] In response to this, the background plasma supplies a return electron current. The spatially overlapping forward and return electron current flows are susceptible to several microinstabilities.[4–11] The current filamentation instability,[12–15] which is often referred to as the Weibel instability,[4] creates a current separation at the length scale of an electron skin depth in the plasma, which leads to a generation of strong magnetic field (~*MGauss*).[16] It is believed that the Weibel instability and its nonlinear evolution are largely responsible for the development of strong magnetic fields in astrophysical contexts like the relativistic shock formation in Gamma ray bursts (GRBs),[17] the high energy cosmic rays,[18,19] active galactic nuclei (AGN)[20] etc. In laser driven laboratory experiments also, Huntington *et al.*[21] have observed

[a]Electronic address: atul.kumar@ipr.res.in
[b]Electronic address: amita@ipr.res.in
[c]Predhiman Kaw is a deceased author.

the ion-Weibel instability in interpenetrating plasma flows. However, the experimental observation of magnetic field generation by the Weibel instability at electron dynamics scale still remains a challenge. In a typical beam plasma system, a fraction of the kinetic energy (δK) associated with the flows get converted into the electromagnetic excitations. Such disturbances feed upon themselves leading to the development of Weibel/current filamentation instabilities.

The energy principle often provides a succinct physical description of the excitations prevalent in any system. It has been regularly adopted for studying the stability of hydrodynamic fluids in a conservative system.[22–27] In plasmas also, the ideal Magnetohydrodynamic (MHD) excitations have often been interpreted using energy principle[28–32] for both equilibria with and without flows. The stability theory with energy principle for ideal magnetohydrodynamics has been employed to study problems in a variety of contexts, e.g. magnetic fusion,[33,34] astrophysics, solar and space physics[35,36] etc. For fast electron time scale phenomena (e.g. the case of beam plasma system) Lashmore-Davis[37] has shown the applicability of energy principle for the electrostatic excitations leading to the two stream instability. Weibel mode is an instability having mixed electrostatic and electromagnetic character. As the wavenumber gets more aligned transverse to the flow direction, electromagnetic character predominates. When it is directed totally orthogonal to the direction of flow, it is also referred to as the current filamentation instability. In this case, the mode has a purely growing character. We have employed the energy principle for this particular configuration. The origin of the positive and negative contributions to the total energy has been clearly identified. The term providing a negative contribution to the energy is responsible for the growth of the mode. The energy conservation, however, should ensure a balance between the positive and negative energy contributions. This condition provides the expression for the growth rate, which is found to be in good agreement with earlier derivations. We have discussed the flow configurations which are more susceptible to the excitation of this mode. It is inferred that a symmetric flow configuration (i.e. when both the beam and the background plasma electrons have identical densities with equal and opposite flow velocities) has the optimal/fastest growth. This is in agreement with results obtained from the linear stability analysis carried out in earlier studies.[12,38]

The manuscript has been organized as follows. Section II describes a model set of equations and presents the derivation of the energetics involved in excitations which are generated in counter-streaming electron currents by a transverse filamentation mode. In section III, the physics inferences obtained from the energy principle have been highlighted. The asymmetry is characterized as the difference between the beam and background electron densities for a charge and current balanced equilibrium configuration. In section IV, the description of the PIC simulation set up has been presented for a comparative study of the symmetric and asymmetric flow configurations. Section V contains the observations and inferences obtained from PIC simulations. Section VI contains the summary.

II. MODEL EQUATIONS AND ENERGETICS

We have considered an equilibrium configuration for a collection of the beam and background plasma electrons flowing in opposite direction to each other against a background of stationary ions. The charge neutrality and the current balance are ensured initially. The charge of the beam and the plasma electron densities are neutralized by the background plasma ions. Thus we have $\sum_\alpha n_{0\alpha} = n_{0i}$, where α is a dummy index which is 1 and 2 representing the beam and plasma electrons respectively. Here, $n_{0\alpha}$ represents the density of the two electron species and n_{0i} is the background density of ions. We will restrict to the 2-D geometry of $x - y$ plane shown in Fig. 1 for our analysis. The beam (depicted by red circles) and background plasma electrons (green circles) are chosen to flow in the $\pm x$ direction respectively. The equilibrium current balance is ensured by choosing $\sum_\alpha n_{0\alpha}\vec{v}_{0\alpha} = 0$, where $\vec{v}_{0\alpha}$ is the equilibrium flow velocity for species 'α'. The system is considered to be of infinite extent in both x and y directions. Such a system in the collisionless limit is in equilibrium with no forces acting on the particles. The total energy of this system is in the form of electron kinetic energy in the beam and the background electrons. Any electromagnetic instability in such a system would develop only if the energy requirement for the growth of electromagnetic fields is compensated by the reduction in the kinetic energy of the electrons.

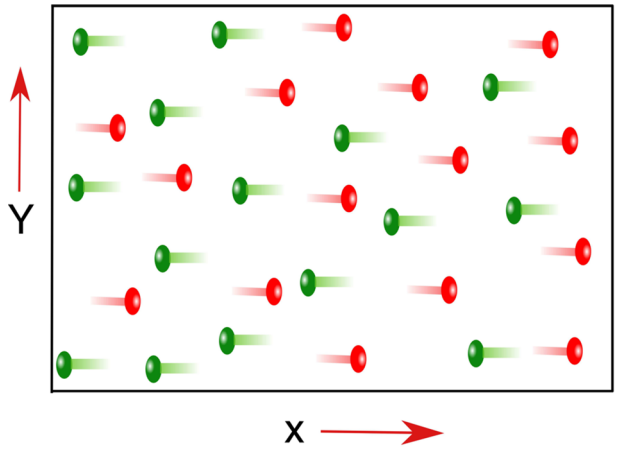

FIG. 1. Schematics of 2-D equilibrium geometry of the beam plasma system where the beam (red circles) and background plasma electrons (green circles) are flowing in positive and negative x direction respectively.

The dynamical evolution of the system about this equilibrium is clearly governed by the coupled set of Maxwell's and electron fluid equations. The ions in this treatment are assumed to be heavy and their response is considered to be negligible. The Maxwell's equations lead to the following equation for the evolution of field energy in the presence of plasma:

$$\frac{\partial}{\partial t}\left(\frac{E^2+B^2}{8\pi}\right)+\frac{c}{4\pi}\vec{\nabla}\cdot(\vec{E}\times\vec{B})+\vec{J}\cdot\vec{E}=0 \tag{1}$$

This is the well known Poynting flux theorem for the electromagnetic energy in the plasma. In the vacuum, $\vec{J}\cdot\vec{E}$ term is absent and the rate of change of electromagnetic energy is determined simply by the Poynting flux. In plasma or any conducting media, the flow of currents leads to a finite value of $\vec{J}\cdot\vec{E}$. This term represents the possibility of energy transfer from the kinetic energy of the particles to the field energy and vice versa. For the infinite system considered by us, the Poynting flux would not contribute to the electromagnetic field energy evolution. We would only have the $\vec{J}\cdot\vec{E}$ term responsible for any rearrangement between field and the kinetic energies. Integrating Eq. (1) over space we obtain:

$$\frac{\partial}{\partial t}\int\left(\frac{E^2+B^2}{8\pi}\right)dxdy+\int\left(\vec{J}\cdot\vec{E}\right)dxdy=0 \tag{2}$$

We now evaluate Eq. (1) for fluctuations excited about the homogeneous equilibrium. Thus, a disturbance in any field is represented by the collection of Fourier modes having the form:

$$f(\vec{r},t)\sim f_k exp(i\vec{k}\cdot\vec{r}-i\omega_k t)+c.c \tag{3}$$

where $c.c$ indicates complex conjugate of the expression to preserve the reality of the left hand side. We consider filamentation instability for which the wavenumber $\vec{k}$ is directed along $\hat{y}$. We represent this component simply by k. For the perturbed current flow confined in 2-D $x-y$ plane, the associated magnetic field is directed along the $\hat{z}$ direction and is denoted by B_{1z}. The perturbed electric field $\vec{E}_1$ lies in the x-y plane. The variations being along $\hat{y}$, E_{1y} is the electrostatic component of the field and E_{1x}, B_{1z} correspond to electromagnetic excitation. These field perturbations are generated as a result of the conversion of the kinetic energy associated with the beam and return electron currents of the system into the electric and magnetic field energies. For the small amplitude linear disturbances, only up to quadratic terms (associated with the perturbed fields) in the energy expression have to be retained. We thus have:

$$\frac{\partial}{\partial t}\left(\frac{E^2+B^2}{8\pi}\right)=\frac{\partial}{\partial t}\left[\frac{1}{8\pi}(E_{1x}^2+E_{1y}^2+B_{1z}^2)\right] \tag{4}$$

$$\vec{J}\cdot\vec{E}=-\sum_{\alpha}\left[en_{0\alpha}v_{1\alpha x}E_{1x}+en_{0\alpha}v_{1\alpha y}E_{1y}+en_{1\alpha}v_{0\alpha}E_{1x}\right] \tag{5}$$

The linearized Maxwell's equations, electron continuity and momentum equations are then used to express Eq. (1) entirely in terms of E_{1x}. We have chosen to normalize time with the inverse of electron plasma frequency, $\omega_{pe} = \sqrt{\frac{4\pi n_0 e^2}{m}}$ and length with the electron skin depth, $d_e = c/\omega_{pe}$ (*i.e.*, $t \cdot \omega_{pe}^{-1} \rightarrow t$ and $y \cdot d_e \rightarrow y$) to obtain the following expression:

$$\frac{1}{8\pi}\frac{\partial}{\partial t}\left[\left(1+\frac{S_2}{\Gamma_k^2}\right)|E_{1xk}|^2 + \left(1+\frac{S_1}{\Gamma_k^2}\right)\frac{S_3^2 k^2}{\Gamma_k^2(\Gamma_k^4 + 2S_1\Gamma_k^2 + S_1^2)}|E_{1xk}|^2 + \frac{k^2}{\Gamma_k^2}|E_{1xk}|^2 - \frac{S_4}{\Gamma_k^4}k^2|E_{1xk}|^2\right] = \frac{\partial}{\partial t}\left[\chi_k\right] = 0 \tag{6}$$

Here, $\omega_k = \omega_{rk} + \iota\Gamma_k$ with ω_{rk} and Γ_k corresponding to the real and imaginary part of ω_k respectively. For the purely growing mode, $\omega_k = \iota\Gamma_k$ where Γ_k represents the growth rate. In addition, we have used the following definitions:

$$S_1 = \sum_\alpha \frac{n_{0\alpha}}{n_0\gamma_{0\alpha}}; \quad S_2 = \sum_\alpha \frac{n_{0\alpha}}{n_0\gamma_{0\alpha}^3}; \tag{7}$$

$$S_3 = \sum_\alpha \frac{n_{0\alpha}v_{0\alpha}}{n_0\gamma_{0\alpha}}; \quad S_4 = \sum_\alpha \frac{n_{0\alpha}v_{0\alpha}^2}{n_0\gamma_{0\alpha}}; \tag{8}$$

The relevant details of the derivation of Eq. (6) have been provided in the Appendix. The parameters S_1, S_2 and S_4 are always positive. It should be noted that though the parameter S_3 can be either positive or negative, it appears only as S_3^2 in Eq. (6). Hence, the sign of S_3 does not matter but its magnitude $|S_3|$ is important. Furthermore, Eq. (6) shows that χ_k (the energy in the kth mode) should remain conserved. This is because in the linear regime the modes do not interact. The system is in a state of equilibrium initially with infinitesimal perturbations around it. Therefore, $\chi_k \approx 0$ for all k initially and from Eq. (6), χ_k would continue to remain zero while the linear approximation remains valid. We thus have:

$$\chi = \frac{1}{8\pi}\left[\left(1+\frac{S_2}{\Gamma^2}\right)|E_{1x}|^2 + \left(1+\frac{S_1}{\Gamma^2}\right)\frac{S_3^2 k^2}{\Gamma^2(\Gamma^4 + 2S_1\Gamma^2 + S_1^2)}|E_{1x}|^2 + \frac{k^2}{\Gamma^2}|E_{1x}|^2 - \frac{S_4}{\Gamma^4}k^2|E_{1x}|^2\right] = 0 \tag{9}$$

In writing Eq. (9), we have dropped the suffix k.

III. INFERENCES FROM ENERGY PRINCIPLE

The expression for χ in Eq. (9) has both positive and negative terms contributing to it which is essential for the existence of any instability in the system. When the positive terms balance with the negative terms to have $\chi = 0$ at a finite value of Γ, the corresponding mode is unstable. The growth rate is thus a function of S_1, S_2, S_3 and S_4, which in turn, are functions of the density and flow parameters of the equilibrium configuration of the beam as well as the background plasma electrons. The first three terms of the expression for χ are positive definite (S_1 and S_2 are positive and S_3 which could be negative, appears as a square). The positive terms require additional energy. The fourth term with a negative sign (S_4 and other factors being positive definite in this term) corresponds to a reduction in energy of the perturbed configuration. The presence of this fourth term is thus energetically favorable and is crucial for instability.

It should be noted here that $\vec{J}\cdot\vec{E} = \sum_\alpha n_\alpha \vec{v}_\alpha \cdot (-e\vec{E})$. Here $-e\vec{E}$ is the force due to the electric field experienced by the electrons. Thus, the positive/negative terms in $\vec{J}\cdot\vec{E}$ represent the gain/loss rate in the kinetic energy of electrons respectively. The negative terms are responsible for the growth of Weibel instability at the expense of the kinetic energy of electrons. We now identify the terms in the expression of $\vec{J}\cdot\vec{E}$ in Eq. (5) which provide a negative contribution to the total energy of the system.

Let us first consider the case of symmetric flow for which S_3 is zero. For this case, it is evident from Eq. (A10) (see Appendix) that $E_{1y} = 0$. Thus, only the first and third term of Eq. (5) are finite for this particular case. Let us now identify their contributions in Eq. (9). The first term of Eq. (9) with the coefficient $(1 + S_2/\Gamma^2)$ of $|E_{1x}|^2$ arises as follows. The coefficient unity clearly comes from $\partial|E_{1x}^2|/\partial t$ of Eq. (4). The term with the factor S_2/Γ^2 is the plasma dressing contribution arising

from $(-\sum_\alpha e n_{0\alpha} v_{1\alpha x} E_{1x})$ (viz. the first term of Eq. (5)). This can be obtained by expressing E_{1x} in terms of $v_{1x\alpha}$ from Eq. (A5) which leads to $(-\sum_\alpha e n_{0\alpha} v_{1\alpha x} E_{1x}) = \sum_\alpha n_{0\alpha} m \gamma_{0\alpha}^3 |v_{1\alpha x}|^2 \Gamma$. Clearly, this is a positive definite and represents the rate of kinetic energy acquired by the electrons due to the perturbed velocity along the $\hat{x}$ direction (i.e. along the equilibrium flow direction). Let us now look at the last term of Eq. (5) by substituting $n_{1\alpha}$ and E_{1x} in terms of the velocities. It is evident from Eq. (A4) that the density perturbations are related to $v_{1\alpha y}$ by the continuity equation. Since E_{1y} is absent for the symmetric flow configuration, $v_{1\alpha y}$ gets generated by the $\vec{v}\times\vec{B}$ force in the momentum equation (Eq. (A3)). It should be noted that since the equilibrium flow is oppositely directed for the two electron fluids, this force acts in the opposite directions for the two species and is responsible for the separation of the two beams transverse to the equilibrium flow direction (i.e. along $\hat{y}$). This causes the spatial separation of the forward and return currents leading to magnetic field generation causing the system to be destabilized by Weibel instability. We substitute for $n_{1\alpha}$ and E_{1x} in terms of v_{1x} to write the last term of Eq. (5) as $-\sum_\alpha k^2 v_{0\alpha}^2 m \gamma_{0\alpha}^3 |v_{1\alpha x}|^2/\Gamma$ which is negative and hence, it represents the loss rate of electron kinetic energy. In Eq. (9), it can be traced as the term with $-S_4 k^2/\Gamma^4$ coefficient.

For asymmetric flows with non zero values of S_3, E_{1y} is finite. A finite value of E_{1y} contributes to $\vec{J}\cdot\vec{E}$ through the second term in Eq. (5) and also through the dependence of $n_{1\alpha}$ on $v_{1\alpha y}$ (Eq. (A4)), which in turn is influenced by the force $-eE_{1y}$ through the momentum equation (Eqs. (A3) and (A6)). It should be noted that the force due to E_{1y} acts on the two fluids along the same direction and hence does not lead to any current separation required for the Weibel destabilization process. The sum of both these terms can be seen to be positive definite and they are responsible for the gain in electron kinetic energy acquired by the perturbed $\hat{y}$ component of the velocity v_{1y}. The term with the coefficient S_1/Γ^2 in Eq. (9) represents the sum of both these contributions. The unity in the bracket containing S_1/Γ^2 arises from $\partial|E_{1y}|^2/\partial t$ of Eq. (4). Furthermore, the term $k^2|E_{1x}|^2/\Gamma^2$ corresponds to the last term of Eq. (4). It also represents the rate of change of the magnetic field energy, $\partial|B_{1z}|^2/\partial t$.

It is, therefore, clear that the negative term arises from the correlation between $n_{1\alpha}$ and E_{1x}, which is the last term appearing in the expression of $\vec{J}\cdot\vec{E}$ (Eq. (5)). This can also be simply viewed as a crucial term reducing the overall spatially averaged perturbed kinetic energy of the electrons as demonstrated below.

$$\left\langle \delta K \right\rangle = \frac{1}{2}\left\langle \sum_\alpha \left[(n_{0\alpha} + n_{1\alpha})(\vec{v}_{0\alpha} + \vec{v}_{1\alpha})^2 - n_{0\alpha} v_{0\alpha}^2 \right] \right\rangle \tag{10}$$

$$= \frac{1}{2}\left\langle \sum_\alpha \left[n_{0\alpha} \vec{v}_{1\alpha}^2 + 2 n_{1\alpha} \vec{v}_{0\alpha}\cdot\vec{v}_{1\alpha} \right] \right\rangle \tag{11}$$

$$= \frac{1}{2}\left\langle \sum_\alpha \left[n_{0\alpha} |v_{1\alpha x}|^2 + n_{0\alpha} |v_{1\alpha y}|^2 + 2 n_{1\alpha} \vec{v}_{0\alpha}\cdot\vec{v}_{1\alpha} \right] \right\rangle \tag{12}$$

It should be noted that the terms linear in perturbation average out to zero and thus have been dropped. The terms with third order in perturbation have been ignored. The first and second terms in Eq. (12) are positive definite. However, the sign of the third term depends on the correlation between $n_{1\alpha}$ and $v_{1\alpha x}$. Using Eq. (A5) and the fact that $\omega = \iota\Gamma$, we end up with the same correlation term as in the expression for $\vec{J}\cdot\vec{E}$ which is responsible for decreasing the kinetic energy.

Now, we derive the expression for the growth rate of the unstable mode. Equating the coefficient of $|E_{1x}|^2$ in Eq. (6) to zero, we obtain the following 6th order polynomial equation as the dispersion relation from which the growth rate can be obtained.

$$(\Gamma^2 + S_1)[\Gamma^4 + (S_2 + k^2)\Gamma^2 - S_4 k^2] = -S_3^2 k^2 \tag{13}$$

Equation (13) is in agreement with earlier derivation.[38] For $S_3 = 0$, the analytical expression for the growth rate can be obtained as:

$$\Gamma = \frac{1}{\sqrt{2}}\left[\sqrt{(S_2 + k^2)^2 + 4 S_4 k^2} - (S_2 + k^2) \right]^{1/2} \tag{14}$$

The other root of $\Gamma^2 = -S_1$ is the electron plasma oscillations. The analytical expression for the growth rate can also be obtained in the asymptotic limit of small beam density, i.e. $n_{01} \ll n_{02}$, $v_{01} \gg v_{02}$ and the beam velocity approaches the speed of light, i.e $|v_{01}| \approx 1$. This implies that $\gamma_{01} = \gamma_0 \gg 1$ and $\gamma_{02} \sim 1$. We can then expand the parameters S_1, S_2, S_3 and S_4 of Eq. (13) in powers of n_{01}. Retaining terms of n_{01} upto first order in the expression we obtain: $S_1 \approx S_2 \approx 1$, $S_3 \approx n_{01}v_{01}$, $S_4 \approx n_{01}v_{01}(v_{01}/\gamma_0 - v_{02})$. The expression for growth rate under this approximation is then given by

$$\Gamma = \left[\frac{k^2 n_{01} v_{01}^2}{(1+k^2)\gamma_0}\right]^{1/2} \tag{15}$$

In the limit $k \ll 1$ the growth rate becomes,

$$\Gamma_1 = (n_{01}v_{01}^2/\gamma_0)^{1/2}k \tag{16}$$

In the other asymptotic limit $k \gg 1$,

$$\Gamma_2 = (n_{01}v_{01}^2/\gamma_0)^{1/2} \tag{17}$$

This is a highly asymmetric flow configuration in which the beam density is much lower than the background plasma density but it has relativistic speeds. The value of $|S_3|$ for such configurations would be very high. On the other hand, $|S_3| = 0$ corresponds to a symmetric flow configuration. This can be understood as follows. Using the condition of charge neutrality $\sum_\alpha n_{0\alpha} = n_0 = 1$ and zero current $\sum_\alpha n_{0\alpha}v_{0\alpha} = 0$ for an equilibrium, we have $n_{01} = 1 - n_{02}$ and $v_{02} = -n_{01}v_{01}/(1 - n_{01})$. All the parameters S_1, S_2, S_3 and S_4, on which the growth rate depends, can then be cast entirely in terms of the beam density and its equilibrium velocity. The parameter S_3 takes the form:

$$S_3 = n_{01}v_{01}\left(\frac{1}{\gamma_{01}} - \frac{1}{\gamma_{02}}\right) \tag{18}$$

Thus, S_3 has a negligible role in non relativistic cases. In the relativistic case, it is zero only when the flow configuration is symmetric. This corresponds to $v_{01} = -v_{02}$, which is possible only when $n_{01} = n_{02} = 0.5$. We will refer to the case of $n_{01} = 0.5$ (corresponding to $|S_3| = 0$) as the 'symmetric' flow configuration and for any other value of n_{01} for which $|S_3|$ is finite the flow configuration is termed as 'asymmetric' henceforth. It is interesting to note from Eq. (A10) that the electrostatic field $E_{1y} = 0$ when $|S_3| = 0$. Thus, for the symmetric flow configuration, no electrostatic field gets generated and hence, it is favorable from the energetics point of view to excite the instability for this particular configuration. In the expression for χ provided in Eq. (9) also, it can be seen that the second positive term vanishes entirely when $|S_3| = 0$. We have carried out a detailed investigation of the growth rate evaluated from the dispersion relation of Eq. (13) in the parameter domain of n_{01} vs. v_{01} to show that this inference drawn from the energy principle is indeed correct.

In Figs. 2(a) and 2(b), we have shown the constant contours of S_4 in the $n_{01} - v_{01}$ plane. When the growth rate using the values of n_{01} and v_{01} on the points of any constant S_4 contour is evaluated, we observe that the growth rate is always highest for the symmetric case. We have employed Eq. (13)

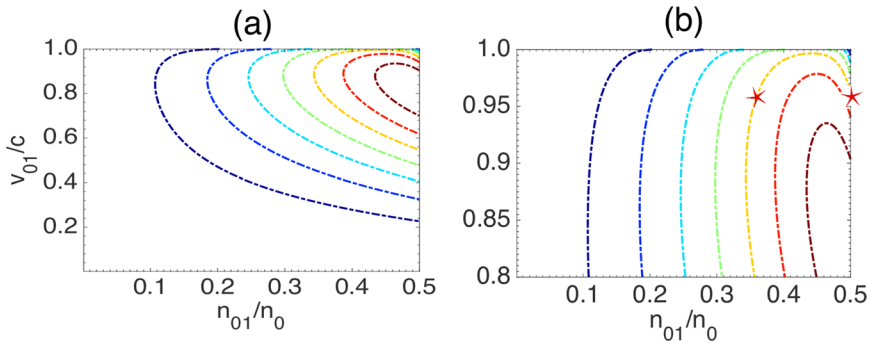

FIG. 2. (a) Contours of S_4 in the plane of n_{01} and v_{01}: (b) zoomed section of contours of S_4 where astricks denote two points of symmetric and asymmetric flow configurations at the constant contour of $S_4 = 0.25$.

TABLE I. The maximum growth rate of current filamentation instability evaluated analytically on a contour of $S_4 = 0.25$.

n_{01}	v_{01}	$\|S_3\|$	Γ(max.)
0.343	0.898	0.1365	0.3748
0.346	0.923	0.1558	0.3722
0.360	0.960	0.1941	0.3636
0.367	0.970	0.2078	0.3581
0.383	0.983	0.2291	0.3475
0.400	0.991	0.2445	0.3336
0.429	0.996	0.2453	0.3258
0.466	0.994	0.1798	0.3857
0.487	0.982	0.0827	0.4392
0.5	0.963	0	0.4519

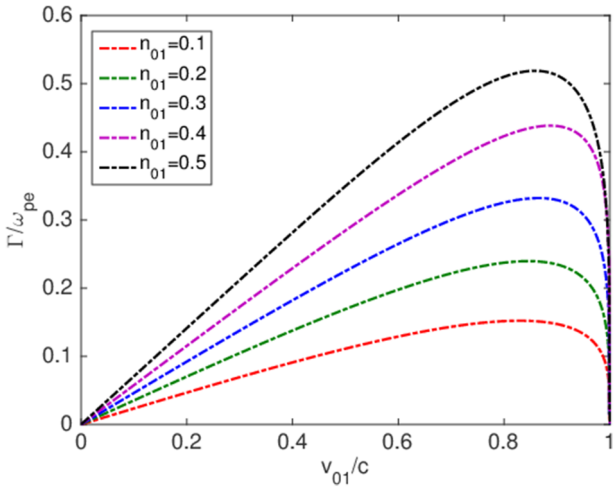

FIG. 3. The equilibrium condition of charge neutrality and zero current requires that only two parameters out of the four $n_{0\alpha}$ and $v_{0\alpha}$ can be chosen independently. For this figure n_{01} and v_{01} have been chosen independently to understand the variation of the growth rate with respect to them. The figure shows the plot of growth rate as a function of v_{01}. Each curve in the plot corresponds to a distinct value of n_{01}. It should be noted that the curve for $n_{01} = 0.5$ representing symmetric flow configuration, has the highest value of growth rate for all values of v_{01}.

to evaluate the growth rate numerically and used $k = 1$ where the growth rate maximizes.[38] In Table I, we have evaluated the growth rate for the constant contours of $S_4 = 0.25$ for various values of n_{01} and v_{01}. We observe that the growth rate is highest for $|S_3| = 0$, as expected. In fact, the growth rate decreases monotonically with increasing value of $|S_3|$.

We have also shown the plot of growth rate for various values of n_{01} as a function of v_{01} in Fig. 3 and observe that the growth rate maximizes when $n_{01} = 0.5$, i.e. for the symmetric flow configuration. It is thus clear that the symmetric flow configuration has the maximum growth rate. It would be interesting to know how the two flow configurations behave in the nonlinear regime. In the next section, we have explored this by carrying out 2-D PIC simulations through OSIRIS for the symmetric and asymmetric flow configurations corresponding to the two points depicted by asterisks in Fig. 2(b). For these two points, both S_4 and v_{01} are identical. Here, Case(A) is for the symmetric flow with $n_{01} = 0.5$, whereas Case (B) is for asymmetric configuration with $n_{01} = 0.36$.

IV. SIMULATION SETUP

PIC simulations using OSIRIS[39,40] have been carried out for a system of the forward electron beam and a compensating return current by the background plasma. The equilibrium configuration in Fig. 1 has been initialized in a 2-D simulation box. The simulation box size was chosen to be

$25c/\omega_{pe} \times 25c/\omega_{pe}$. The spatial resolution is taken to be 50 cells per c/ω_{pe} with 64 particles per cell which corresponds to a grid size of $\Delta x = 0.02c/\omega_{pe}$ and time step $\Delta t = 0.012\omega_{pe}^{-1}$. A small noise in terms of initial thermal velocity of $v_{th} = 0.0001397c$ in each of the two electron species has been introduced initially. In typical beam plasma experiments, one envisages the forward beam current to have high velocities and low density. On the other hand, the background plasma electrons have high density and move with slower speed. Thus the two flows would, in general, be highly asymmetric. We investigate here both the cases of symmetric and asymmetric flows. For a proper comparison, we have ensured in the choice of the equilibrium flow parameters to have identical values of S_4 as well as the beam velocity v_{01} for both the cases. For the symmetric flow (**Case** (**A**)), a forward moving beam of density $0.50n_0$ moving with the velocity of $0.963c$ and a compensating return electron beam with same density and speed moving in opposite direction has been chosen. For asymmetric flow (**Case** (**B**)), a beam electron density of $0.36n_0$ moving along $\hat{x}$ with a velocity of $0.960c$ in the forward direction and a shielding current of background electrons along $-\hat{x}$ with density $0.64n_0$ moving with a velocity of $0.540c$ has been considered. We have tracked the spatio - temporal evolution of magnetic field and particle density along with the evolution of total magnetic field energy in the system defined by $\frac{1}{8\pi}\int B^2(x,y)dxdy$.

V. SIMULATION RESULTS

We have shown in Fig. 4, the evolution of the normalized magnetic field energy in the system for Case (A) and (B) respectively. It can be observed from the semilog plot of Fig. 4 that the magnetic field energy grows linearly in the beginning. However, the symmetric flow *i.e*, Case (A) shows a higher growth rate than that of Case (B), as expected. The field energy in Case (A) also saturates at a higher value. The 2-D color plots for the z component of the magnetic field (left column) and the charge density (right column) for Case (A) and Case (B) have been shown in Figs. 5 and 6 respectively. The first subplot in both the figures [Figs. 5 and 6] corresponds to the linear regime. After this, the system shows the onset of nonlinear effects. This can be clearly observed from the plots in Fig. 4 where the lines start to curve. This happens for Case (A) and Case (B) at $t = 15.24$ and $t = 18.0$ respectively. At the linear stage of instability ($t = 15.24$ in Fig. 5 and $t = 18.0$ in Fig. 6), the formation of filaments in the magnetic field as well as in the electron charge density are observed.

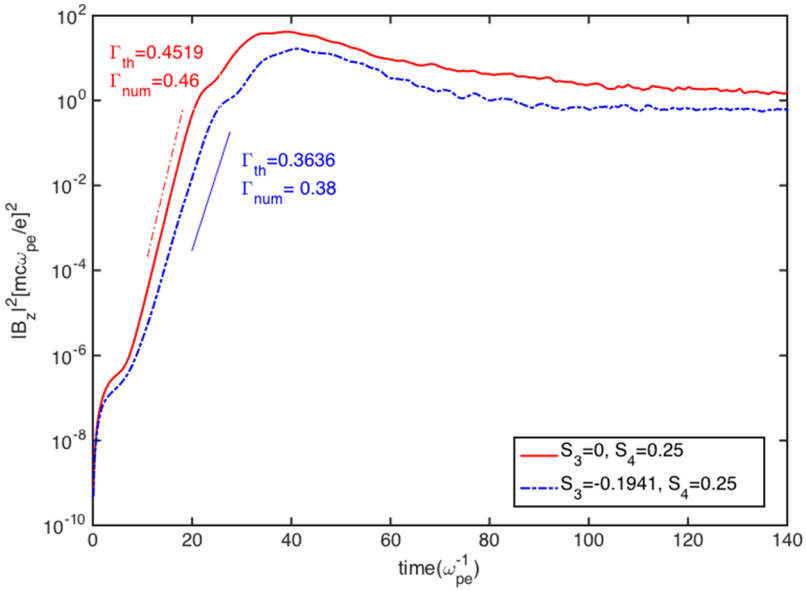

FIG. 4. The calculation of growth rate of instability by its slope on temporal evolution of magnetic field energy for the symmetric ($S_4 = 0.25$, $|S_3| = 0$) (solid red color curve) and asymmetric flow ($S_4 = 0.25$, $|S_3| = 0.1941$) (dotted blue curve) which match very well with the theoretical growth rate.

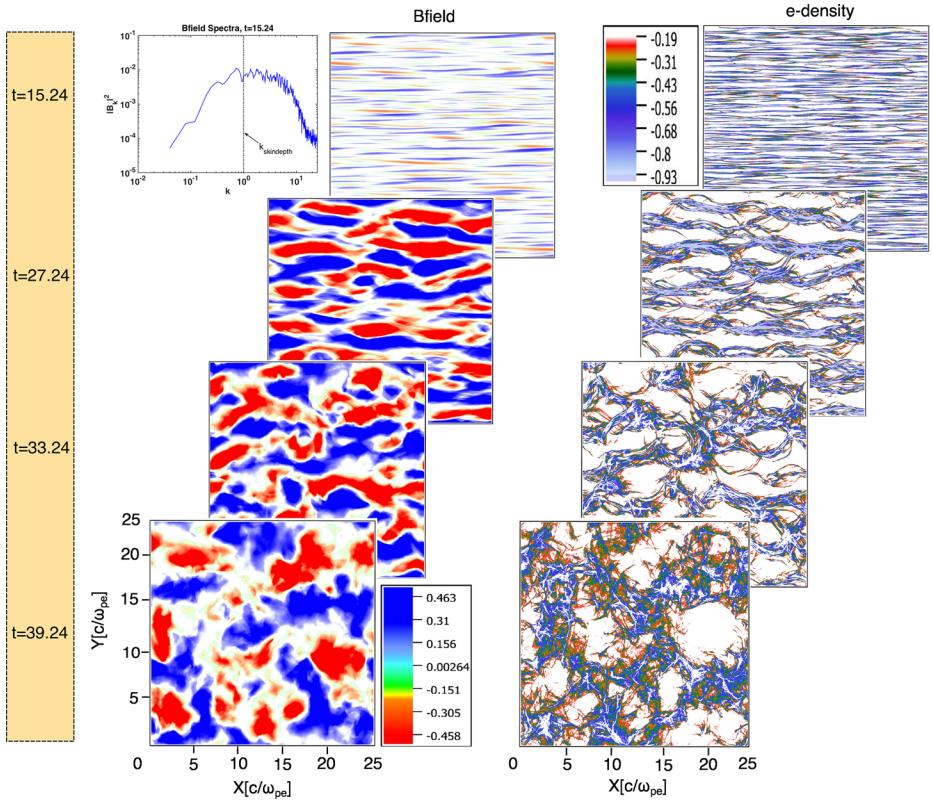

FIG. 5. Evolution of magnetic field (left column) and electron charge density of the beam (right column) for symmetric flows (prepared by Vapor [J. Clyne *et al.*, New Journal of Physics **9**, 8 (2007); J. Clyne and M. Rast, Electronic Imaging, 284–295 (2005)]): The formation of filamentary structures in magnetic field as well as in electron charge density at the order of an electron skin depth, d_e is shown just at the transition from linear to nonlinear stage (t=15.24). In the nonlinear stage of instability, the tilted structure of filaments in the magnetic field as well as in electron charge density which is a signature of oblique mode instability, can be seen. The magnetic field energy spectra in the linear regime peaking at d_e is shown with in the top left corner of the figure. Further evolution of instability leads to the system in a turbulent regime which is caused by the deflection of charge particles due to a high amplitude magnetic field generated by the instability in the system.

The scale length of these filaments are of the order of electron skin depth d_e. However, the magnitude of the perturbed magnetic field in the asymmetric case is comparatively much weaker. It is evident from Eq. (6) that finite value of $|S_3|$ (which is the case for asymmetric plasma flows) can stabilize the growth of Weibel instability as compared to the system of symmetric plasma flows ($|S_3| = 0$). The slope corresponding to the numerically evaluated growth rate has been indicated by the short straight lines alongside the two respective cases. They show a good match in the linear regime of numerical simulation. The quantitative value of the growth rate calculated by PIC simulation is $\Gamma_{num} = 0.46$ which is in good agreement with theoretical growth rate [Eq. (14)] $\Gamma_{th} = 0.4519$ (red solid color in Fig. 4). In the case of asymmetric flow ($|S_3| = 0.1941$), the growth rate obtained from simulation is $\Gamma_{num} = 0.38$ which also matches with the theoretical result [Eq. (13)] $\Gamma_{th} = 0.3636$ (dotted blue color line) and confirms the theoretical prediction that non-zero value of $|S_3|$ reduces the growth rate of Weibel instability. It should, however, be noted that analytical derivation corresponds to the filamentation configuration with perturbation wave vector directed transverse to the flow direction. However, the simulation shows variations along the flow direction as well, for both the cases. The slight difference between analytical and simulation growth rate is reasonable as the oblique modes are the ones which supposedly dominate the beam plasma instability. However, since the variations along the flow direction are of much longer scales, they do not seem to influence the growth rate much. This is the reason for a good agreement between the analytically evaluated growth rate and that obtained from simulation.

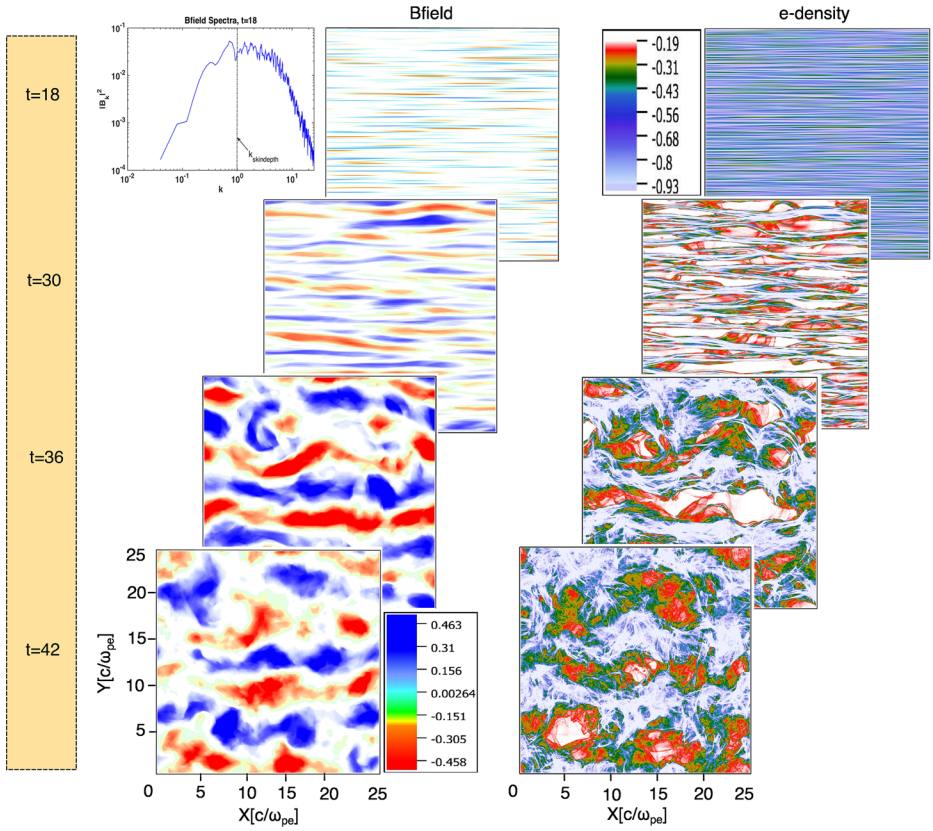

FIG. 6. Evolution of magnetic field (left column) and electron charge density (right column) of the beam for asymmetric flow (prepared by Vapor [J. Clyne *et al.*, New Journal of Physics **9**, 8 (2007); J. Clyne and M. Rast, Electronic Imaging, 284–295 (2005)]): In the asymmetric flows, the term $|S_3|\neq 0$ stabilizes the system, therefore the growth rate of instability reduces as compared to symmetric flow. The nonlinear phase of the instability, therefore, has a slow onset.

It has also been found in our simulations that the nonlinear onset of Weibel instability occurs sooner (just after $t = 15.24$) in Case (A) than in Case (B) ($t = 18.0$). The nonlinear saturation level in Case (A) is also typically higher as compared to Case (B).

In the nonlinear regime, the perturbed magnetic field first keeps increasing at a slower rate (phase 1). The magnetic field structures during this time coalesce and form longer scale structures. Thus, a cascade of power towards longer scales is distinctly observed. The energy evolution plots of Fig. 4, also show a subsequent later regime (phase 2) in which the magnetic energy shows a steady decrease. The color subplots of Fig. 5 at $t = 27.24$ and $t = 39.24$ for Case (A) correspond to these two distinct nonlinear phases. For Fig. 6 the subplot at $t = 30.0$ and $t = 42.0$ depicts the two nonlinear phases for Case (B). During the first phase of the nonlinear regime, the filamentary nature of the structures continues to exist as can be seen from Figs. 5 and 6. Thus, variations along the propagation direction continue to remain at longer spatial scales. In this regime, the coalescence of magnetic filaments increases the transverse scale length. In the second phase of the nonlinear regime, the magnetic structures start to isotropize as can be observed from the last two subplots of Figs. 5 and 6.

VI. SUMMARY

The energy principle utilizes the energy cost associated with the perturbed equilibria to ascertain whether the growth of a particular mode is energetically favorable or not. This technique often provides an interesting physical insight and has been extensively employed in the context of plasma systems governed by Magnetohydrodynamics. Recently, it has been invoked for understanding the electrostatic two stream instability.

In this study, we have shown that an energy principle argument can be put forth for the electromagnetic Weibel mode in the context of beam plasma system. The perturbations in linear regime provide both positive and negative energy contributions in the system. This is essential for the instability, as for conservative system the total energy of the system is constant. The system should allow the possibility of the growth of perturbations without any additional cost of energy. This can happen only when the perturbations merely transfer energy from one form to another. Thus causing one form of energy to grow at the cost of another. For the beam filamentation instability, the electromagnetic field energy in the perturbed state grows at the cost of kinetic energy of the equilibrium flow. We have identified $S_4 = \sum_\alpha \frac{n_{0\alpha} v_{0\alpha}^2}{n_0 \gamma_{0\alpha}}$ as the coefficient of the negative energy contributing term and is crucial for the instability. We have also shown that a finite value of $S_3 = \sum_\alpha \frac{n_{0\alpha} v_{0\alpha}}{n_0 \gamma_{0\alpha}}$ is responsible for generating the electric field transverse to the flow profile and in fact, costs energy. It is clear that S_3 is finite only in the relativistic case and for the case when the flow profile is asymmetric (beam and background plasma have different densities). The finite value of S_3 suppresses the filamentation mode. This has been verified by comparing the growth rates for various cases in this manuscript. For instance, it has been shown that for a constant value of S_4 the growth rate is maximum for $|S_3| = 0$ and reduces monotonically with increasing value of $|S_3|$. We have also carried out 2-D PIC simulations to illustrate the difference between symmetric and asymmetric flow configurations. We have chosen two flow parameters for which S_4 is same. The value of S_3 is zero for one case and is finite for the other case corresponding to symmetric and asymmetric configurations respectively. We have observed that even in the presence of 2-D perturbations (permitted by the 2-D PIC simulations carried out by us) the symmetric case has higher growth rate. Furthermore, the nonlinear saturation level of the perturbed magnetic field is also observed to be higher for the symmetric flow configuration.

It is interesting to note that the parameters (e.g. S_3 and S_4) responsible for the growth rate of the Weibel/current filamentation instability in the infinite system considered here, change their roles for destabilizing a beam plasma system when the beam has a finite transverse extent. In this case, Poynting flux becomes relevant and contributes to the negative energy excitations. This has been shown in a recent submission.[41]

APPENDIX:

We provide here the important steps in the derivation of Eq. (6). The linearized continuity equation for the species α can be written as:

$$\frac{\partial n_{1\alpha}}{\partial t} + \frac{\partial}{\partial y}(n_{0\alpha} v_{1\alpha y}) = 0 \tag{A1}$$

Similarly, linearizing the x and y components of momentum equation for the species α we have:

$$\frac{\partial}{\partial t}(m\gamma_{0\alpha}^3 v_{1\alpha x}) = -eE_{1x}; \tag{A2}$$

$$\frac{\partial}{\partial t}(m\gamma_{0\alpha} v_{1\alpha y}) = -eE_{1y} + ev_{0\alpha} B_{1z}; \tag{A3}$$

where 'e' is the magnitude of the electronic charge and 'm' is the rest mass of an electron. Employing the Fourier representation of Eq. (3) for the linearized fields (density, velocity, electric and magnetic field), we can cast the Eqs. (A1)–(A3) to obtain:

$$n_{1\alpha} = \frac{k}{\omega} n_{0\alpha} v_{1\alpha y} \tag{A4}$$

$$v_{1\alpha x} = -\frac{\iota e}{m\gamma_{0\alpha}^3 \omega} E_{1x} \tag{A5}$$

$$v_{1\alpha y} = -\frac{\iota e}{m\gamma_{0\alpha} \omega} E_{1y} - \frac{\iota e}{m\gamma_{0\alpha} \omega^2} k v_{0\alpha} E_{1x} \tag{A6}$$

Here, we have omitted the suffix k from the Fourier representation of the fields. The Faraday's law gives the following relationship between the $\hat{z}$ component of magnetic field and the $\hat{x}$ component of electric field:

$$B_{1z} = -\frac{k}{\omega} E_{1x} \tag{A7}$$

The Poisson's equation can be written as:

$$\frac{\partial E_{1y}}{\partial y} = -\sum_{\alpha} 4\pi e n_{1\alpha} \tag{A8}$$

Using Eqs. (A4)–(A6), we can express the Poisson equation as:

$$\iota k E_{1y} = -\sum_{\alpha} 4\pi e \frac{k}{\omega} n_{0\alpha}\left[-\frac{\iota e}{m\gamma_{0\alpha}\omega} E_{1y} - \frac{\iota e}{m\gamma_{0\alpha}\omega^2} k v_{0\alpha} E_{1x}\right] \tag{A9}$$

Rearranging terms in Eq. (A9) along with the definition of S_1 and S_3 provided in Eqs. (7) and (8), we can cast E_{1y} in terms of E_{1x} as:

$$E_{1y} = \frac{\omega_{pe}^2 S_3}{(1 - \frac{\omega_{pe}^2}{\omega^2} S_1)\omega^3} E_{1x} \tag{A10}$$

It should be noted that when $S_3 = 0$, we have $E_{1y} = 0$. Thus a symmetric flow configuration for which S_3 vanishes does not generate any electrostatic field and hence, the energy cost in this case for the development of Weibel mode is less. We eliminate all the other fields in terms of E_{1x} and use the normalized variables, i.e. $\omega/\omega_{pe} \rightarrow \omega$ and $kc/\omega_{pe} \rightarrow k$ to obtain:

$$\begin{aligned}
\vec{J}\cdot\vec{E} = {} & \frac{\iota}{8\pi}\left[S_2\left\{\frac{1}{\omega} - \frac{1}{\omega_*}\right\}\right]|E_{1x}|^2 \\
& + \frac{\iota}{8\pi}\left[\frac{S_3^2 S_1 k^2}{|\omega|^6(1-\frac{1}{\omega^2}S_1)(1-\frac{1}{\omega_*^2}S_1)}\left\{\frac{1}{\omega} - \frac{1}{\omega_*}\right\} + \frac{S_3^2 k^2}{|\omega|^4}\left\{\frac{1}{\omega_*(1-\frac{1}{\omega_*^2}S_1)} - \frac{1}{\omega(1-\frac{1}{\omega^2}S_1)}\right\}\right]|E_{1x}|^2 \\
& + \frac{\iota}{8\pi}\left[S_3^2 k^2\left\{\frac{1}{\omega^5(1-\frac{1}{\omega^2}S_1)} - \frac{1}{\omega_*^5(1-\frac{1}{\omega_*^2}S_1)}\right\} + S_4 k^2\left\{\frac{1}{\omega^3} - \frac{1}{\omega_*^3}\right\}\right]|E_{1x}|^2
\end{aligned} \tag{A11}$$

The above expression can be simplified to write:

$$\vec{J}\cdot\vec{E} = \frac{2\Gamma}{8\pi}\left[\frac{S_2}{\Gamma^2} + \frac{S_1 S_3^2 k^2}{\Gamma^4(\Gamma^4 + 2S_1\Gamma^2 + S_1^2)} - \frac{S_4}{\Gamma^4}\right]|E_{1x}|^2 \tag{A12}$$

$$= \frac{1}{8\pi}\frac{\partial}{\partial t}\left[\frac{S_2}{\Gamma^2} + \frac{S_1 S_3^2 k^2}{\Gamma^4(\Gamma^4 + 2S_1\Gamma^2 + S_1^2)} - \frac{S_4}{\Gamma^4}\right]|E_{1x}|^2 \tag{A13}$$

It should be noted that we have replaced 2Γ by $\partial/\partial t$ because $E_{1x} = E_{1xk}\ exp(iky - i\omega t)$. Thus $|E_{1x}|^2 \sim exp(2\Gamma t)$. Here, Γ is the imaginary part of the frequency ω. Similarly, we have:

$$\begin{aligned}
\frac{\partial}{\partial t}\left(\frac{E^2 + B^2}{8\pi}\right) &= \frac{1}{8\pi}\frac{\partial}{\partial t}\left[\left\{1 + \frac{k^2 S_3^2}{|\omega|^6(1-\frac{1}{\omega^2}S_1)(1-\frac{1}{\omega_*^2}S_1)} + \frac{k^2}{|\omega|^2}\right\}\right]|E_{1x}|^2 \\
&= \frac{1}{8\pi}\frac{\partial}{\partial t}\left[\left\{1 + \frac{S_3^2 k^2}{\Gamma^2(\Gamma^4 + 2S_1\Gamma^2 + S_1^2)} + \frac{k^2}{\Gamma^2}\right\}\right]|E_{1x}|^2
\end{aligned} \tag{A14}$$

Since the Poynting flux for the homogeneous infinite periodic system is zero, we can express Eq. (1) by summing Eqs. (A13) and (A14), to obtain Eq. (6).

[1] A. Modena, Z. Najmudin, A. Dangor, C. Clayton, K. A. Marsh, C. Joshi, V. Malka, C. Darrow, C. Danson, D. Neely, and F. N. Walsh, "Electron acceleration from the breaking of relativistic plasma waves," Nature **377**, 606–608 (1995).

[2] F. Brunel, "Anomalous absorption of high intensity subpicosecond laser pulses," Physics of Fluids **31**(9), 2714 (1988).

[3] K. B. Wharton, S. P. Hatchett, S. C. Wilks, M. H. Key, J. D. Moody, V. Yanovsky, A. A. Offenberger, B. A. Hammel, M. D. Perry, and C. Joshi, "Experimental measurements of hot electrons generated by ultraintense laser-plasma interactions on solid-density targets," Phys. Rev. Lett. **81**, 822–825 (1998).

[4] E. S. Weibel, "Spontaneously growing transverse waves in a plasma due to an anisotropic velocity distribution," Phys. Rev. Lett. **2**, 83–84 (1959).

[5] O. Buneman, "Dissipation of currents in ionized media," Phys. Rev. **115**, 503–517 (1959).

[6] T. F. Bell and O. Buneman, "Plasma instability in the whistler mode caused by a gyrating electron stream," Phys. Rev. **133**, A1300–A1302 (1964).
[7] K. V. Roberts and H. L. Berk, "Nonlinear evolution of a two-stream instability," Phys. Rev. Lett. **19**, 297–300 (1967).
[8] E. A. Startsev and R. C. Davidson, "Two-stream instability for a longitudinally compressing charged particle beam," Physics of Plasmas **13**(6), 062108 (2006).
[9] A. Bret, "Weibel, two-stream, filamentation, oblique, bell, buneman... which one grows faster?," Astrophysical Journal **699**(2), 990–1003 (2009).
[10] A. Das and P. Kaw, "Nonlocal sausage-like instability of current channels in electron magnetohydrodynamics," Physics of Plasmas **8**(10), 4518–4523 (2001).
[11] C. Shukla, A. Das, and K. Patel, "Particle-in-cell simulation of two-dimensional electron velocity shear driven instability in relativistic domain," Physics of Plasmas **23**(8), 082108 (2016).
[12] F. Pegoraro, S. V. Bulanov, F. Califano, and M. Lontano, "Nonlinear development of the weibel instability and magnetic field generation in collisionless plasmas," Physica Scripta **T63**(3), 262–265 (1996).
[13] A. Bret, M. C. Firpo, and C. Deutsch, "Characterization of the initial filamentation of a relativistic electron beam passing through a plasma," Physical Review Letters **94**(11), 1–4 (2005).
[14] A. Bret, L. Gremillet, and M. E. Dieckmann, "Multidimensional electron beam-plasma instabilities in the relativistic regime," Physics of Plasmas **17**(12) (2010).
[15] W. Fox, G. Fiksel, A. Bhattacharjee, P. Y. Chang, K. Germaschewski, S. X. Hu, P. M. Nilson, T.-c. Lai, S. X. Luan, W. Yu, F. Y. Li, D. Wu, Z. M. Sheng, M. Y. Yu, and J. Zhang, "Filamentation instability of counterstreaming laser-driven plasmas," Physical Review E - Statistical, Nonlinear, and Soft Matter Physics **111**(22), 1–5 (2013).
[16] S. Mondal, V. Narayanan, W. J. Ding, A. D. Lad, B. Hao, S. Ahmad, W. M. Wang, Z. M. Sheng, S. Sengupta, P. Kaw, A. Das, and G. R. Kumar, "Direct observation of turbulent magnetic fields in hot, dense laser produced plasmas," Proceedings of the National Academy of Sciences **109**(21), 8011–8015 (2012).
[17] I. F. Mirabel and L. F. Rodriguez, "Sources of relativistic jets in the galaxy," Annual Review of Astronomy and Astrophysics **37**(1), 409–443 (1999).
[18] A. R. Bell, "The acceleration of cosmic rays in shock fronts—I," Monthly Notices of the Royal Astronomical Society **182**(2), 147 (1978).
[19] M. Ackermann, M. Ajello, A. Allafort, L. Baldini, J. Ballet, G. Barbiellini, M. G. Baring, D. Bastieri, K. Bechtol, R. Bellazzini, R. D. Blandford, E. D. Bloom, E. Bonamente, A. W. Borgland, E. Bottacini, T. J. Brandt, J. Bregeon, M. Brigida, P. Bruel, R. Buehler, G. Busetto, S. Buson, G. A. Caliandro, R. A. Cameron, P. A. Caraveo, J. M. Casandjian, C. Cecchi, Ö. Çelik, E. Charles, S. Chaty, R. C. G. Chaves, A. Chekhtman, C. C. Cheung, J. Chiang, G. Chiaro, A. N. Cillis, S. Ciprini, R. Claus, J. Cohen-Tanugi, L. R. Cominsky, J. Conrad, S. Corbel, S. Cutini, F. D'Ammando, A. de Angelis, F. de Palma, C. D. Dermer, E. do Couto e Silva, P. S. Drell, A. Drlica-Wagner, L. Falletti, C. Favuzzi, E. C. Ferrara, A. Franckowiak, Y. Fukazawa, S. Funk, P. Fusco, F. Gargano, S. Germani, N. Giglietto, P. Giommi, F. Giordano, M. Giroletti, T. Glanzman, G. Godfrey, I. A. Grenier, M.-H. Grondin, J. E. Grove, S. Guiriec, D. Hadasch, Y. Hanabata, A. K. Harding, M. Hayashida, K. Hayashi, E. Hays, J. W. Hewitt, A. B. Hill, R. E. Hughes, M. S. Jackson, T. Jogler, G. Jóhannesson, A. S. Johnson, T. Kamae, J. Kataoka, J. Katsuta, J. Knödlseder, M. Kuss, J. Lande, S. Larsson, L. Latronico, M. Lemoine-Goumard, F. Longo, F. Loparco, M. N. Lovellette, P. Lubrano, G. M. Madejski, F. Massaro, M. Mayer, M. N. Mazziotta, J. E. McEnery, J. Mehault, P. F. Michelson, R. P. Mignani, W. Mitthumsiri, T. Mizuno, A. A. Moiseev, M. E. Monzani, A. Morselli, I. V. Moskalenko, S. Murgia, T. Nakamori, R. Nemmen, E. Nuss, M. Ohno, T. Ohsugi, N. Omodei, M. Orienti, E. Orlando, J. F. Ormes, D. Paneque, J. S. Perkins, M. Pesce-Rollins, F. Piron, G. Pivato, S. Rainò, R. Rando, M. Razzano, S. Razzaque, A. Reimer, O. Reimer, S. Ritz, C. Romoli, M. Sánchez-Conde, A. Schulz, C. Sgrò, P. E. Simeon, E. J. Siskind, D. A. Smith, G. Spandre, P. Spinelli, F. W. Stecker, A. W. Strong, D. J. Suson, H. Tajima, H. Takahashi, T. Takahashi, T. Tanaka, J. G. Thayer, J. B. Thayer, D. J. Thompson, S. E. Thorsett, L. Tibaldo, O. Tibolla, M. Tinivella, E. Troja, Y. Uchiyama, T. L. Usher, J. Vandenbroucke, V. Vasileiou, G. Vianello, V. Vitale, A. P. Waite, M. Werner, B. L. Winer, K. S. Wood, M. Wood, R. Yamazaki, Z. Yang, and S. Zimmer, "Detection of the characteristic pion-decay signature in supernova remnants," Science **339**(6121), 807–811 (2013).
[20] A. H. Bridle, "Sidedness, field configuration, and collimation of extragalactic radio jets," Astron. J **89**, 979–986 (1984).
[21] C. M. Huntington, F. Fiuza, J. S. Ross, A. B. Zylstra, R. P. Drake, D. H. Froula, G. Gregori, N. L. Kugland, C. C. Kuranz, M. C. Levy, C. K. Li, J. Meinecke, T. Morita, R. Petrasso, C. Plechaty, B. A. Remington, D. D. Ryutov, Y. Sakawa, A. Spitkovsky, H. Takabe, and H.-S. Park, "Observation of magnetic field generation via the Weibel instability in interpenetrating plasma flows," Nature Physics **11**(2), 173–176 (2015).
[22] I. B. Bernstein, E. A. Frieman, M. D. Kruskal, and R. M. Kulsrud, "An energy principle for hydromagnetic stability problems," Proceedings of the Royal Society of London A: Mathematical, Physical and Engineering Sciences **244**(1236), 17–40 (1958).
[23] E. Frieman and M. Rotenberg, "On hydromagnetic stability of stationary equilibria," Rev. Mod. Phys. **32**, 898–902 (1960).
[24] R. Kulsrud, "General stability theory in plasma physics," in *Advanced Plasma Theory* (M. N. Rosenbluth, ed.), Vol. 1, p. 54, 1964.
[25] M. B. Isichenko, "Nonlinear hydrodynamic stability," Phys. Rev. Lett. **80**, 972–975 (1998).
[26] E. Hameiri, "Variational principles for equilibrium states with plasma flow," Physics of Plasmas **5**(9), 3270–3281 (1998).
[27] P. A. Davidson, "An energy criterion for the linear stability of conservative flows," Journal of Fluid Mechanics **402**, 329–348 (2000).
[28] G. Laval, C. Mercier, and R. Pellat, "Necessity of the energy principles for magnetostatic stability," Nuclear Fusion **5**(2), 156 (1965).
[29] J. Freidberg, *Ideal magnetohydrodynamics* (Plenum Press, New York, NY, 1987).
[30] E. Hameiri, "Dynamically accessible perturbations and magnetohydrodynamic stability," Physics of Plasmas **10**(7), 2643–2648 (2003).

[31] A. V. Kats, "Canonical description of ideal magnetohydrodynamic flows and integrals of motion," Phys. Rev. E **69**, 046303 (2004).
[32] I. V. Khalzov, A. I. Smolyakov, and V. I. Ilgisonis, "Energy of eigenmodes in magnetohydrodynamic flows of ideal fluids," Physics of Plasmas **15**(5), 054501 (2008).
[33] J. W. V. Dam, M. N. Rosenbluth, and Y. C. Lee, "A generalized kinetic energy principle," The Physics of Fluids **25**(8), 1349–1354 (1982).
[34] A. Bhattacharjee, R. L. Dewar, A. H. Glasser, M. S. Chance, and J. C. Wiley, "Energy principle with global invariants: Applications," The Physics of Fluids **26**(2), 526–534 (1983).
[35] R. M. Kulsrud and J. W. K. Mark, "Collective instabilities and waves for inhomogeneous stellar systems. I. The necessary and sufficient energy principle," The Astrophysical Journal **160**(May), 471–484 (1970).
[36] J. P. Goedbloed, "Variational principles for stationary one- and two-fluid equilibria of axisymmetric laboratory and astrophysical plasmas," Physics of Plasmas **11**(12), L81–L84 (2004).
[37] C. N. Lashmore-Davies, "Two-stream instability, wave energy, and the energy principle," Physics of Plasmas **14**(9), 092101 (2007).
[38] F. Califano, R. Prandi, F. Pegoraro, and S. V. Bulanov, "Nonlinear filamentation instability driven by an inhomogeneous current in a collisionless plasma," Phys. Rev. E **58**, 7837–7845 (1998).
[39] R. A. Fonseca, L. O. Silva, F. S. Tsung, V. K. Decyk, W. Lu, C. Ren, W. B. Mori, S. Deng, S. Lee, T. Katsouleas, and J. C. Adam, *OSIRIS: A Three-Dimensional, Fully Relativistic Particle in Cell Code for Modeling Plasma Based Accelerators* (Springer Berlin Heidelberg, Berlin, Heidelberg, 2002), pp. 342–351.
[40] R. A. Fonseca, S. F. Martins, L. O. Silva, J. W. Tonge, F. S. Tsung, and W. B. Mori, "One-to-one direct modeling of experiments and astrophysical scenarios: Pushing the envelope on kinetic plasma simulations," Plasma Physics and Controlled Fusion **50**(12), 124034 (2008).
[41] A. Das, A. Kumar, C. Shukla, R. K. Bera, D. Verma, B. Patel, Y. Hayashi, K. A. Tanaka, A. Lad, G. R. Kumar, and P. Kaw, "Evidence of new finite beam plasma instability for magnetic field generation," e-print arXiv:1712.03099v1[physics.plasm-ph], pp. 0–9, 2017.